3 Biotech (2020) 10:214
https://doi.org/10.1007/s13205-020-02205-5

ORIGINAL ARTICLE

Decolorization and biodegradation of textile di-azo dye Acid Blue 113 by *Pseudomonas stutzeri* AK6

Anjali U. Joshi[1] · Ankit T. Hinsu[1] · Rohitkumar J. Kotadiya[1] · Jalpa K. Rank[1] · Kavan N. Andharia[1] · Ramesh K. Kothari[1]

Received: 14 August 2019 / Accepted: 12 April 2020

Abstract
Textile industry is one of the anthropogenic activities that consume a large amount of water and pollute water bodies. It uses a massive amount of dyes, which is one of the main constituents of polluting textile effluent. In the present research, biodegradation of Acid Blue 113 dye, a commonly used textile di-azo dye, has been studied exploiting *Pseudomonas stutzeri*, strain AK6. The dye (300 ppm) was decolorized up to 86.2% within 96 h. The metabolites of Acid Blue 113 obtained after biodegradation were identified by various analytical techniques viz. HPLC (high-performance liquid chromatography) and GC–MS (gas chromatography–mass spectrometry). Genome analysis of isolate AK6 using IMG/M (Integrated Microbial Genomes and Microbiomes) system supported the role of azoreductase and laccase for the decolorization and degradation of azo dye. The ability of *P. stutzeri* AK6 to tolerate high amount of dye makes it a potential candidate for bioremediation and pre-processing to remove dyes from textile effluents.

Keywords Textile dyes · Biodegradation · *Pseudomonas stutzeri* · Azoreductase · Laccase

Introduction

The textile industry occupies a unique position in Indian economy, contributing towards industrial production, employment and exports (Chavan 2001). However, the wastewater discharged from this industry has become a continuous source of environmental pollution, as it contains synthetic dyes which exert harmful effects on the environment and living organisms (Ulson et al. 2010).

Azo dyes form the largest class of aromatic synthetic dyes, having one or more –N=N– (azo) bonds and are used extensively in textile, cosmetics, paper, food, and pharmaceutical industry, with textile industry as its largest consumer (Alalewi and Jiang 2012). During the dyeing process, 2% (basic dyes)–50% (reactive dyes) dyes are lost from the fabric (O'Neill et al. 1999; Pandey et al. 2007). The addition of dye-contaminated wastewater in aquatic ecosystems causes serious problems like obstruction in light penetration, reduction of oxygen transfer and toxic effects on aquatic flora–fauna (Solís et al. 2012). Dyes have been known to mankind since ancient times (Vankar 2016); however, synthetic dyes were manufactured in the late nineteenth century, causing high incidences of bladder cancer due to dye intermediates benzidine and 2-naphthylamine (Christie 2007). Diseases such as dermatitis and disorders of the central nervous system (Khan and Malik 2018), as well as inactivation of enzymatic activities (Copaciu et al. 2013) are caused due to textile dyes. Workers in textile industry also face a major risk due to carcinogenic, mutagenic and toxic effects of textile dyes (Aquino et al. 2014; Khatri et al. 2018). All these factors make the treatment of wastewater containing dyes necessary before its discharge into water bodies or being used for irrigation purposes.

Various methods such as coagulation, flocculation, activated carbon adsorption and reverse osmosis, based on physical and chemical approaches, are being used for the treatment of colored textile effluent. Among these methods, ozonation, coagulation, flocculation, and electrochemical methods have resulted in poor color removal

Electronic supplementary material The online version of this article (https://doi.org/10.1007/s13205-020-02205-5) contains supplementary material, which is available to authorized users.

✉ Ramesh K. Kothari
kothari1971@gmail.com; rkkothari@sauuni.ac.in

[1] UGC-CAS Department of Biosciences, Saurashtra University, Rajkot, Gujarat 360005, India

Published online: 25 April 2020

and reverse osmosis is not cost-effective (O'Neill et al. 1999). Besides, the chemicals used in these techniques are costly and give rise to secondary pollutants (Jadhav et al. 2007). Moreover, the treatment of textile effluent with these techniques leads to transmission of dye from one phase to another, thus leaving the problem mostly unsolved. So, there is a great need to develop an economical and effective way of dealing with textile dyeing waste. Biological remediation of dye pollution is a better option, as microorganisms are genetically diverse and metabolically resourceful (Banat et al. 1997; Robinson et al. 2001).

In addition to this, biological treatment presents a relatively inexpensive and environment-friendly alternative, producing less sludge and requires lesser number of reagents. Besides being economical, it can lead to the complete mineralization of dyes (Pandey et al. 2007; Enayatzamir et al. 2009). Sludge is used as inoculum for the biological treatment of textile effluents containing dyes (Khalid et al. 2009). Many microbial species and strains have emerged as candidates for use in bioaugmentation, notably *Enterobacter* sp. CV–S1 (Roy et al. 2018), *Alishewanella* sp. CBL-2 (Ajaz et al. 2018), *Alcaligenes aquatilis* (Ajaz et al. 2019), *Shewanella putrefaciens* (Khalid et al. 2008), genetically engineered *E. coli* JM109 (Jin et al. 2008), etc.

Acid Blue 113 is a commercially crucial di-azo dye used for dyeing wool, silk, leather, paper, and polyamide fibre. Degradation of this dye has gained momentum during the last few years. In the present study, a di-azo dye (dye containing two –N=N– azo bonds) degrading bacterium, *Pseudomonas stutzeri* strain AK6, was examined for its efficiency for bioremediation by using complete genome analysis and degradation studies.

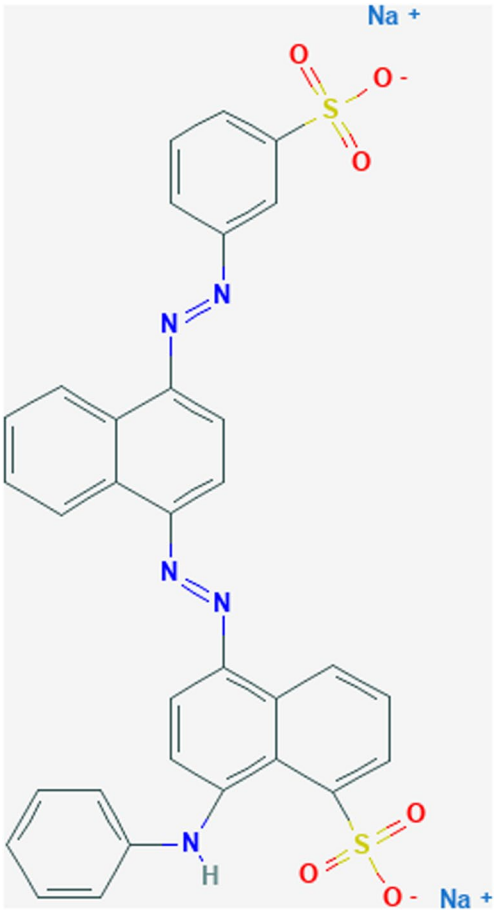

Fig. 1 Chemical structure of Acid Blue 113 dye (Source: https://pubchem.ncbi.nlm.nih.gov/compound/18776)

Materials and methods

Sample collection

Textile effluent was collected from the point of discharge at a dye manufacturing industry located in GIDC (21.6180° N, 73.0228° E), Ankleshwar, Gujarat, India. The sample was transported to the laboratory and stored at 4 °C until use.

Dyes and media

Acid Blue 113 (Fig. 1), was obtained from the textile industry situated at Ankleshwar, Gujarat, India. Bushnell and Haas medium (BHM) (Bushnell and Haas 1941) and other medium requirements and chemicals were procured from HiMedia laboratories Ltd. (Mumbai).

Isolation and identification of dye-decolorizing bacteria

Textile effluent (10 mL) was added to 100 mL BHM [(gL^{-1}): $MgSO_4$ 0.2; K_2HPO_4, 1.0; $CaCl_2$, 0.02; $FeCl_3$, 0.05; NH_4NO_3, 1.0] supplemented with glucose (0.1% w/v), yeast extract (0.3% w/v) and dye (500 ppm) to enrich dye-decolorizing and degrading bacteria. After 3 days, 10 mL of enriched culture was added to fresh enrichment medium, incubated at 37 °C for 72 h, and a loopful of enriched culture was streaked on N-agar and incubated at 37 °C. Morphologically different bacterial isolates were purified and stored on N-agar slants. Earlier reports suggest that co-substrates such as glucose and yeast extract are required to donate the electrons for the reduction of azo-bonds by bacteria (Chan et al. 2011).

Properties of the bacterial isolates

Morphological and biochemical identification of the bacterial strain was performed with the help of Gram's staining and VITEK® 2 system (BioMérieux, France).

Decolorization assay and spectral scan

Bushnell and Haas Broth (BHB), 30 mL in 100 mL Erlenmeyer's flask, along with glucose (0.1% w/v) and yeast extract (0.3% w/v) and 300 ppm dye, was inoculated with active bacterial culture (5%) and incubated at 37 °C under static culture condition in triplicate. The absorbance and decolorization rate were determined from 5.0 mL samples withdrawn at an interval of 24, 48, 72, and 96 h after incubation. Culture aliquots were centrifuged (Eppendorf, Germany) at 12,857×*g* or 10,000 rpm for 10 min. Decolorization of dye was determined by monitoring the decrease in absorbance at 561 nm wavelength using a spectrophotometer (Analytik Jena, Germany) as described previously (Mehta et al. 2011). Uninoculated BHM supplemented with dye was used as control. Average decolorization rate was calculated as per previous reports (Parshetti et al. 2006) and given as:

$$\text{Decolorization rate } (\%) = A - \frac{B}{A} \times 100,$$

where A is the initial absorbance and B the observed absorbance.

$$\text{Average decolourization rate} = C \times D\% \times 1000/100 \times t,$$

where C is the initial concentration of dye, $D\%$ is the dye decolorized, and t is the time in hours.

The supernatant filtrates were scanned with a range of wavelengths (λ, 400 to 800 nm) on a spectrophotometer (Analytik Jena, Germany).

Extraction of treated dye products

Bushnell and Haas Broth (BHB), 750 mL in 2000 mL Erlenmeyer's flask, along with glucose (0.1% w/v) and yeast extract (0.3% w/v) and 300 ppm dye, was inoculated with the active bacterial culture (5%) and incubated at 37 °C under static culture condition. After 96 h, the decolorized medium was centrifuged at 12,857×*g* or 10,000 rpm for 10 min, and an equal volume of ethyl acetate was added to the supernatant, vigorously mixed for 2 h and allowed to settle overnight. The ethyl acetate layer was collected separately and evaporated after the removal of aqueous content with anhydrous Na_2SO_4 in a rotary evaporator, dried at 40 °C and used for further analysis (Ghodake et al. 2011).

HPLC (high-performance liquid chromatography) analysis

Degradation analysis by HPLC was carried out at room temperature by using a slightly modified method reported by Ghodake et al. (2011). Water's Acquity UPLC equipped with BSM, PDA detector, and SM auto-injector and C18 column (Sunfire C18 150 * 4.6 mm, 5 µm) was used. Sample (2 µL) was injected, and dye products were allowed to separate for 10 min at the flow rate of 0.5 mL/min. For the study of Acid Blue 113, methanol:water 50:50 mobile phase was used and the UV–Vis detector was set at 254 nm.

GC–MS (gas chromatography–mass spectrometry) analysis

A QP2010 Ultra spectrometer (Shimadzu) at ionization voltage 70 eV and a single quadrupole analyzer were used to perform GC–MS. Gas chromatography was conducted in the temperature programming mode with a Rxi-5 ms column (30 m * 0.25 µm * 0.25 mm). The initial column temperature was 40 °C for 2 min, then increased linearly at 10 °C/min, to 320 °C and held for 2 min. Split injection mode (split ratio: 20:1) was used and the temperature of the injection port was 310 °C and the GC–MS interface was maintained at 330 °C. The helium carrier gas flow rate was 0.80 mL/min, with a total run time of 30 min. This method was adopted with slight modifications in the GC–MS analysis used by Ghodake et al. (2011). The metabolites of the Acid Blue 113 dye degradations were identified and confirmed using ChemDraw Ultra 12.0 (Soft 2001).

Genome analysis of the bacterial isolate

Genomic DNA was extracted from an activated culture in nutrient broth using the method given by Keiser et al. (2000). Further, DNA was treated with RNAse A (Thermo Fisher, CA) to remove RNA contamination. The quality and quantity of DNA were checked with agarose gel electrophoresis and Nanodrop, respectively. The paired-end sequencing library was prepared using Illumina TruSeq Nano DNA Library preparation kit (Illumina, CA) as per manufacturer's instructions. Sequencing was carried out on Illumina Nextseq 500 (Illumina, CA) machine using 2 × 150 bp chemistry at a commercial facility (Eurofins genomics India Pvt. Ltd., Bangalore, India).

All the raw reads were quality filtered using prinseq-lite script using Q30 cutoff. All the filtered reads were assembled using SPAdes v3.10 (Bankevich et al. 2012), CLC Genomics Workbench v7.0 (QIAGEN, Germany), Celera assembler v8.3 (Denisov et al. 2008) and VelvetOptimiser 2.2.5 (Zerbino and Birney 2008). All these assemblies were then integrated into a single assembly using CISA 1.3 (Lin

and Liao 2013) incorporated within MyPro pipeline (Liao et al. 2015). Further, QUAST v2.3 (Gurevich et al. 2013) was used to evaluate different assemblies, and CheckM (Parks et al. 2015) was utilized to check the completeness of the assembled genome. Assemblies merged with CISA were found to be better than the rest (based on longer assembly length, lesser number of scaffolds, a higher value of N50) and considered for further analysis.

The assembly was submitted at NCBI under the accession number PZYR00000000 and annotation was done using NCBI Prokaryotic Genome Annotation Pipeline (PGAP) (Tatusova et al. 2016) during submission. RDP-naïve Bayesian classification and BLAST with 16 s rRNA database was done to check the identity of the organism. Complete proteome was used to construct whole genome-based phylogenetic trees without sequence alignment by using a Composition Vector (CV) approach using CV-Tree v3.0 (Qi et al. 2004; Zuo and Hao 2015). Further, the genome, along with annotation from PGAP was submitted to IMG/M server and analyzed with other genomes present in IMG/M. Specifically, genes involved in decolorization and degradation (laccase, azo reductase) were searched and compared based on their Pfam and COG domains among all the *P. stutzeri* genomes available in IMG/M (Tables S1). All other analysis, including average nucleotide identity (ANI), comparison of sequences, phylogenetic tree construction, were performed with IMG/M.

Results and discussion

Isolation and identification of di-azo dye bacterial isolate

Several bacterial isolates have been reported, which show remarkable ability to decolorize dyes such as Acid Blue 113 (Park et al. 2005; Pillai 2017). *P. stutzeri* was specifically reported to decolorize direct black, congo red and gentian violet (Bafana et al. 2007; Kuppusamy et al. 2017). The majority of the dye-degrading organisms are *Pseudomonas,* which have a diverse set of degrading capabilities. Many researchers (Kadam et al. 2011; Dutta et al. 2014; Predescu and Nicolae 2012) have earlier reported approximately 10–200 mg L^{-1} dye concentration in the textile effluent. Therefore, 500 ppm dye concentration was used to enrich organisms that were able to withstand high toxicity levels as well as degrade the dye. Primary screening studies resulted in the isolation of six different bacterial isolates (data not shown) based on the decolorization of the enrichment medium inoculated with dye (500 ppm). Each bacterial isolate was checked for its individual decolorization ability and the bacterial isolate AK6 was selected based on its consistent and maximum decolorization capacity of Acid Blue 113 (data not shown) and studied further.

The isolate AK6 was found to be a rod-shaped Gram-negative aerobe that was able to utilize cellulose and starch (Figure S1). It shows a positive result for TSI agar slant, indicating the production of acid and gas during metabolism. The isolate AK6 shows a positive result for tyrosine aryl amidase (Table S2). The bacterial isolate AK6 was identified as *Pseudomonas stutzeri* based on its 16 s rRNA gene (discussed further in genome characterization). *P. stutzeri* is found in abundance in almost all environments globally and possesses a high degree of physiological and genetic adaptability. It shows great metabolic flexibility, which is constant with a large, effective population size. Similar to other *Pseudomonas* species (e.g., *P. putida*), *P. stutzeri* is also involved in environmentally important activities such as N_2 fixation, metal cycling and degradation of biogenic and xenobiotic compounds like oil derivatives, aromatic and non-aromatic hydrocarbons and biocides. *P. stutzeri* is an opportunistic, but rare pathogen (Lalucat et al. 2006). Well-characterized strains such as *P. stutzeri* YC-YH1 are able to degrade pesticides (Shi et al. 2015); *P. stutzeri* KF716 utilizes biphenyl as a sole source of carbon and energy and degrades polychlorinated biphenyls (Hirose et al. 2015); *P. stutzeri* AN10 (CCUG 29243) is a model strain for aerobic naphthalene degradation (Brunet-Galmés et al. 2012); *P. luteola* XLDN4-9 (CCTCC M 205094) and *P. stutzeri* XLDN-R (CCTCC AB 2012149) are able to degrade carbazole (Liu et al. 2012); *P. stutzeri* strain B1SMN1 degrades naphthalene and simultaneously fixes nitrogen (Busquets et al. 2013), and *P. stutzeri* ODKF13 is studied for its naphthalene degradation and nitrogen fixation pathways and for its characterization as an organophosphate degrader of phosphotriester and phosphorothioate insecticides (Iyer and Damania 2016). In accordance with all these strains, the newly isolated AK6 strain was able to decolorize di-azo dye and degrade naphthalene. Similar to its closest neighbour strain, ODKF13, AK6 can fix N_2.

Decolorization study of Acid Blue 113 by isolate AK6

Pseudomonas stutzeri strain AK6 showed remarkable dye-decolorizing property with 86.2% decolorization of Acid Blue 113 (300 ppm) within 96 h under static culture conditions with an average decolorization rate of 3635 µg/h. It could also tolerate extremely high dye concentrations of around 1100 ppm. UV–visible spectroscopy confirms color removal for Acid Blue 113 without the appearance of a new peak (Fig. 2). Similar reports were confirmed for the degradation of Amaranth dye by *Acinetobacter calcoaceticus* NCIM 2890 (Ghodake et al. 2011).

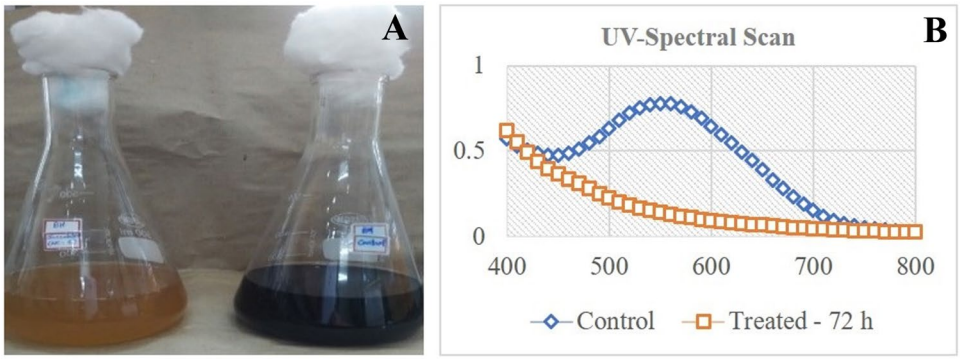

Fig. 2 **a** Decolorization of Acid Blue 113 with isolate AK6. Left flask shows decolorized media after 96 h, while right flask is the control flask. **b** UV–Visible spectrum of Acid Blue 113 (100 ppm) at 0 h and 72 h

Analysis of degraded dye products

HPLC chromatogram (Fig. 3a) showed a peak at retention time 2.665 min, and the solvent extract of the decolorized media showed the appearance of eight new peaks at retention time 2.731, 3.082, 3.337, 4.141, 4.602, 5.622, 6.222 and 7.814 (Fig. 3b). These results indicate the breakdown of Acid Blue 113 dye and the formation of some new metabolites in the treated dye.

Further, GC–MS analysis confirmed the formation of primary and secondary amines (Fig. 4). The degradation products of the Acid Blue 113 were identified as sodium-4-aminobenzene sulfonate (Fig. 4a), sodium-4- amino, 1-naphthyl benzene sulfonate (Fig. 4b) and sodium-5-amino-8-anilino naphthalene 1-sulfonate (Fig. 4c). Based on the observed metabolites in the degraded product, the presence of azoreductase and laccase enzyme was suspected for the cleavage of an azo bond.

Different groups of bacteria decolorize various azo dyes under anaerobic, facultatively anaerobic, and aerobic conditions (Chang and Kuo 2000). Under aerobic culture conditions, bacteria catalyze the incorporation of oxygen into the aromatic ring of organic compounds before ring fission (Sarayu and Sandhya 2010). After the reduction of azo compounds with oxygen-catalyzed azo reductases, the aerobic bacteria produce aromatic amines (Lin et al. 2010). The aerobic azo reductases use both NAD(P)H and NADH as cofactors and reductively cleave carboxylated

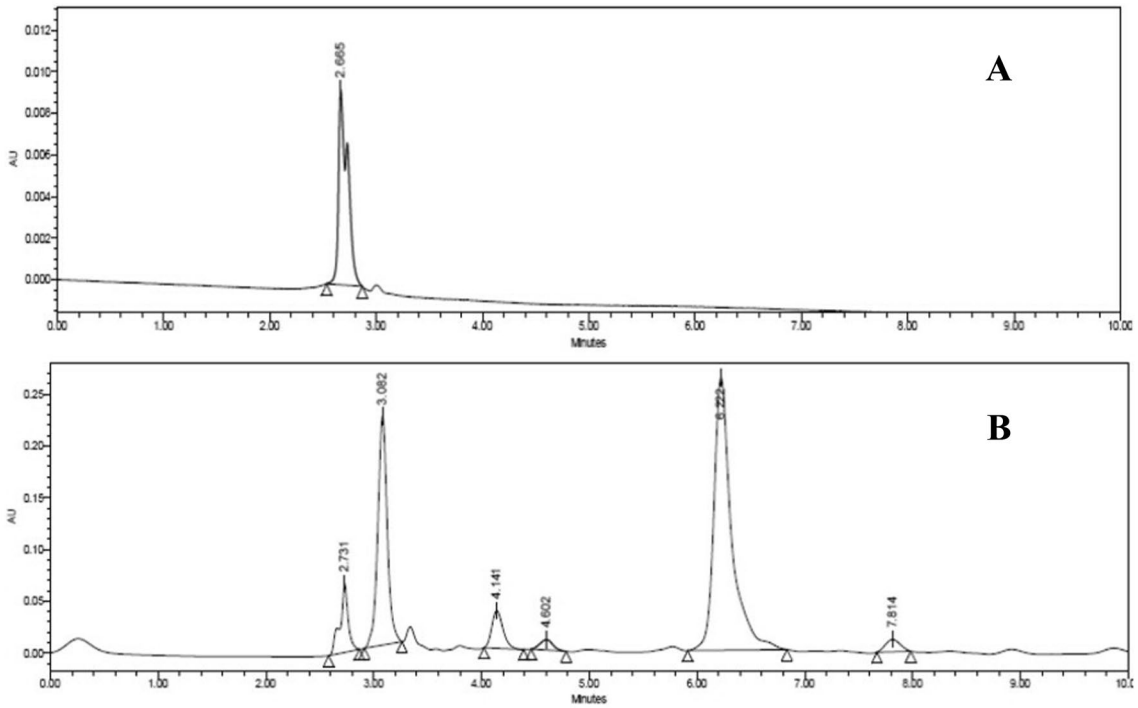

Fig. 3 HPLC elution profiles of **a** Acid Blue 113 native dye, **b** metabolites of Acid Blue 113 dye after its biodegradation

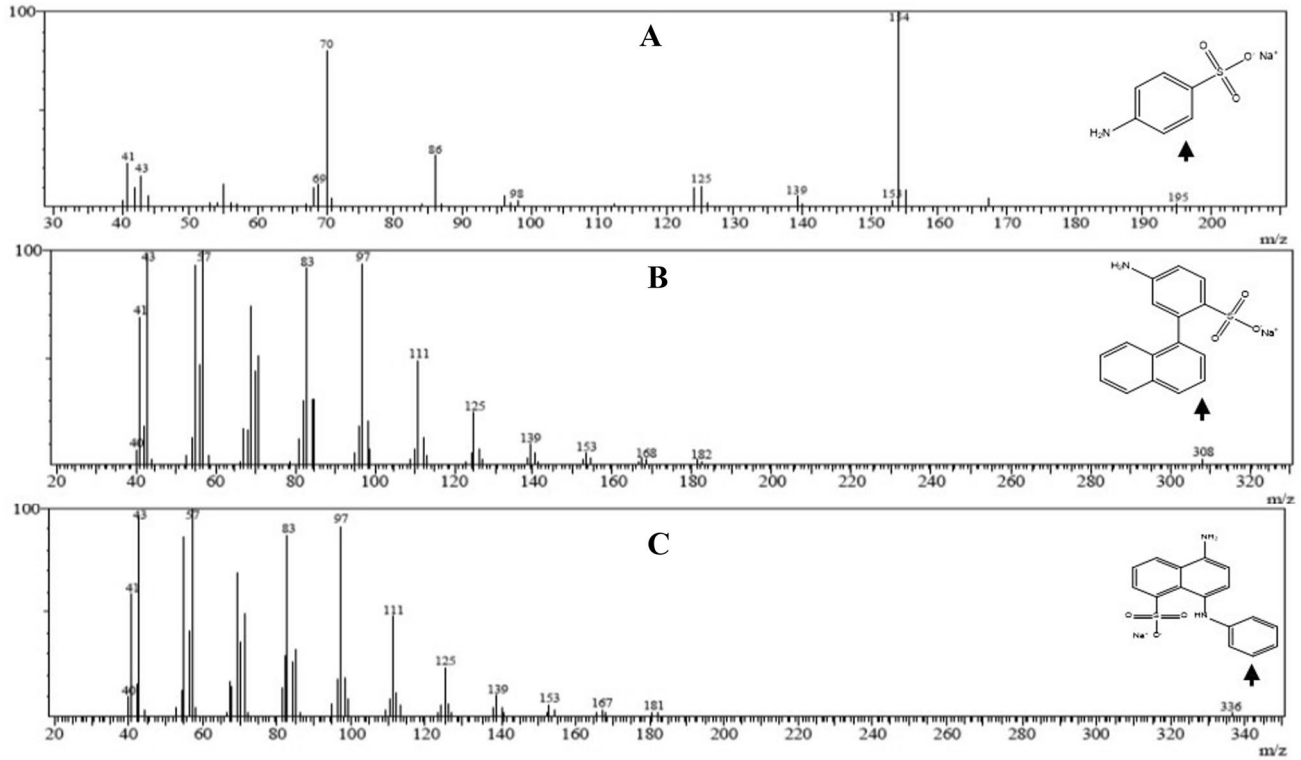

Fig. 4 GC–MS spectral mass peaks of biodegradation products of Acid Blue 113 dye identified as **a** sodium-4-aminobenzene sulfonate, m/z—195, **b** sodium-4-amino, 1-naphthyl benzene sulfonate, m/z—308, **c** sodium-5-amino-8-anilino naphthalene 1-sulfonate, m/z—336

growth substrates of the bacteria and the sulfonated structural analogs (Nachiyar and Rajakumar 2005).

On the other hand, laccases (E.C.1.10.3.2), also known as phenol oxidase, are copper-containing enzymes that catalyze the oxidation of several aromatic and inorganic substances (particularly phenols), along with the reduction of oxygen to water (Majcherczyk et al. 1998). The mode of action of laccases for decolorization of azo dyes is through a highly non-specific free radical mechanism to avoid the formation of toxic aromatic amines (Kalme et al. 2009). Earlier studies have demonstrated that azo bonds are broken first during the degradation of azo dyes (Chen et al. 2005). The presence of azoreductase and laccase genes in the genome of AK6 was observed. From this, the breakage of azo bonds in the dye was predicted.

Further, all the possible metabolites after breakage (Fig. 5) were identified in the results of GC–MS. The presence of laccase and azoreductase was also supported by laccase assay using 0.216 mM syringaldazine (Bhavsar et al. 2018) and azoreductase assay (Nachiyar and Rajakumar 2005), respectively (data not shown). The presence of the above enzymes is also supported by the structure of the degraded dye products.

Genome characterization of the bacterial isolate AK6

Whole-genome sequencing of the bacterial isolate AK6 yielded a total of 1.07 GB high-quality data, which were considered for downstream analysis. The final genome consisted of 30 scaffolds amounting to 4.416 Mb with 64% GC content and N50 of 290,503 bp (Table 1) with completeness and contamination of 100% and 13.66%, respectively. Two approaches were used to identify the bacterial isolate based on 16 s rRNA identification, i.e., RDP-naïve Bayesian classification and BLAST with NCBI 16 s rRNA database. The former confirmed the isolate to be *Pseudomonas* with 99% accuracy, and the latter confirmed the isolate to be *Pseudomonas stutzeri* (99% identical to *Pseudomonas stutzeri* strain ATCC 17588). Additionally, whole proteome-based phylogeny placed isolate AK6 closest to *P. stutzeri* A1501 (Figure S2). Average nucleotide identity (ANI) calculated among all *P. stutzeri* available in IMG/M was in the range of 69.1–98.1% and showed the highest identity with *P. stutzeri* ODKF13 (98.1%) (Table 2). Since closely related organism *P. stutzeri* ODKF13 and many other *P. stutzeri* can degrade naphthalene, we also checked the same in isolate AK6 and

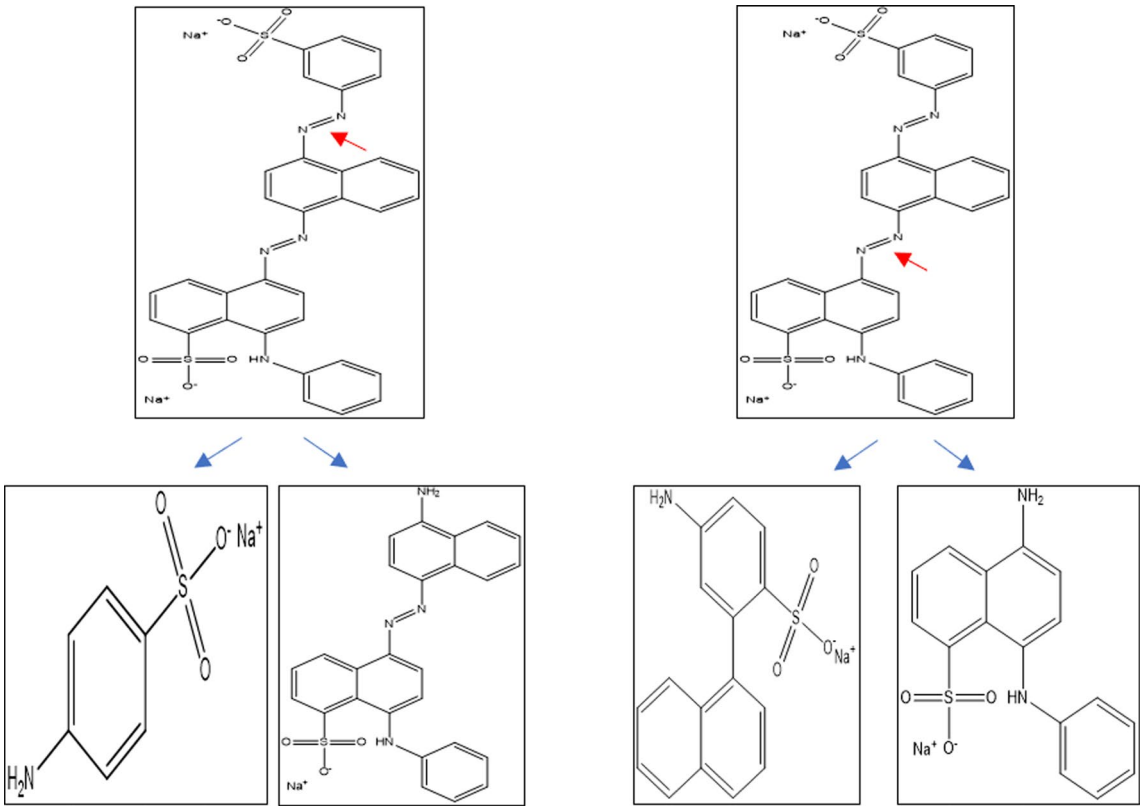

Fig. 5 Formation of new metabolites from Acid Blue 113 dye. Red arrow indicates the breakage of azo bonds

Table 1 Assembly statistics from various software

	Spades	Celera	CLC	Velvet	CISA
# contigs	50	45	59	61	30
Largest contig	412,629	552,630	412,497	412,567	561,268
Total length	4,407,895	4,394,359	4,398,159	4,394,909	4,416,401
N50	281,243	217,782	244,249	212,736	290,503

observed that AK6 also possesses naphthalene degradation ability (data not shown).

Annotation using NCBI-PGAP predicted 4092 protein-coding genes, 104 pseudogenes, and 59 RNA genes, including 5 rRNA genes (1, 5 s rRNA; 1, 16 s rRNA, and 3, 23 s rRNA) and 51 tRNA genes. It was also predicted to be an auxotroph for L-lysine, L-histidine, and L-leucine. The presence of genes coding amylase and cellulase was detected in IMG/M. It was also confirmed experimentally on media containing starch and cellulose as the sole carbon source (data not shown).

Based on the GC–MS reports of the treated dye metabolites, the actions of azoreductase and laccase enzymes were predicted. These genes were searched in the genome of AK6 and compared with all available *P. stutzeri* in IMG/M (31 including AK6) based on the Pfam and COG domains within IMG/M (Table 3). A single copy of azoreductase gene was identified based on the Pfam domain (pfam02525) and COG domain (COG1182) annotated as FMN-dependent NADH-azoreductase in AK6. Additionally, 34 other azoreductases were observed among all *P. stutzeri*. Azoreductase from AK6 showed the highest similarity with *P. stutzeri* NT0124 (isolated from wheat rhizosphere) (99.6%) and *P. stutzeri* XLDN-R (a carbazole-degrading strain) (99.2%).

Laccase is a member of the multicopper oxidase family, which catalyzes the oxidation of substituted phenolic and non-phenolic compounds in the presence of oxygen as an electron acceptor. A total of 138 genes containing Cu oxidase domain were identified among all *P. stutzeri*. All *P. stutzeri* isolates contained a single copy of multicopper oxidase-4 domain-containing gene (annotated as hypothetical protein in all isolates) (pfam02578) (total 31 genes). Just like other *P. stutzeri*, isolate AK6 also contained multicopper oxidase with three cupredoxin domain gene

Table 2 Average nucleotide identity (ANI) of *P. stutzeri* AK6 with all available *P. stutzeri* (named as Genome 2) isolates in IMG/M

Genome2 IMG/M ID	Genome2 Name	ANI (AK6 to Genome 2)	ANI (Genome 2 to AK6)
2651869923	*P. stutzeri* NP_8HO	69.11	69.18
2684623063	*P. stutzeri* 273	79.85	79.84
2565956579	*P. stutzeri* 28a24	79.96	79.97
2651869922	*P. stutzeri* NP_8Ht	79.98	79.95
2516653030	*P. stutzeri* SDM-LAC	80.12	80.11
2648501367	*P. stutzeri* NT0128	80.23	80.23
2524614740	*P. stutzeri* MF28	80.78	80.78
2519899778	*P. stutzeri* JM3000, DSM 10701	82.09	82.08
2630968662	*P. stutzeri* YC-YH1	82.55	82.56
2645727761	*P. stutzeri* KF716	84.18	84.17
2531839177	*P. stutzeri* TS44	84.35	84.33
2529293194	*P. stutzeri* ZoBell 632, ATCC 14405	86.55	86.55
2519899602	*P. stutzeri* KOS6	86.83	86.82
2574179801	*P. stutzeri* 19SMN4	87.24	87.24
2518645567	*P. stutzeri* AN10, CCUG 29243	87.32	87.32
2507149015	*P. stutzeri* RCH2	87.4	87.41
2648501316	*P. stutzeri* ST-9	87.47	87.46
2713897178	*P. stutzeri* BAL361	87.48	87.49
2546826726	*P. stutzeri* ASK-1	87.62	87.61
2537562078	*P. stutzeri* NF13	87.76	87.76
2740892126	*P. stutzeri* HI00D01	90.39	90.38
650716077	*P. stutzeri* CGMCC 1.1803	97.55	97.55
2516653029	*P. stutzeri* XLDN-R	97.75	97.75
651053060	*P. stutzeri* CMT.A.9, DSM 4166	97.88	97.88
2541047503	*P. stutzeri* B1SMN1	97.89	97.88
640427133	*P. stutzeri* A1501	97.89	97.89
2671180787	*P. stutzeri* C2	98	98
2516653031	*P. stutzeri* T13	98.1	98.09
2654587733	*P. stutzeri* NT0124	98.12	98.11
2728369572	*P. stutzeri* ODKF13	98.14	98.13

(includes cell division protein FtsP and spore coat protein CotA) (pfam07731 and pfam07732) and copper-resistance protein family CopA gene (pfam00394, pfam07731, and pfam07732). However, both these genes were present in a single copy, unlike most of the *P. stutzeri,* which has duplications. Multicopper oxidase-4 domain-containing gene, multicopper oxidase with three cupredoxin domain genes and copper-resistance protein family CopA gene from AK6 showed the highest homology with *P. stutzeri* XLDN-R (99.6%), *P. stutzeri* C2 (99.8%) and *P. stutzeri* CGMCC 1.1803 (99.3%), respectively. Further, 12 other isolates harbored dissimilatory nitrite reductase gene containing pfam domains pfam00127, pfam07731, and pfam07732, which was missing in our isolate AK6. pfam00127 (bacterial azurin family of copper binding proteins), which includes pseudoazurin from *Pseudomonas*, was not detected in the genome of our isolate.

Conclusion

The bacterial isolate AK6, identified as *P. stutzeri,* was able to decolorize 86.2% Acid Blue 113 dye (300 ppm) within 96 h. The degradation analysis of the treated dye using analytical techniques like UV–visible spectroscopy, HPLC, and GC–MS confirmed the breakdown of the dye by AK6 bacterium. Further, genome analysis of the isolate defined the presence of genes for the enzymes laccase and azo-reductase, which have been reported for the degradation of various azo dyes. The bacterial isolate can further be assessed for degradation of other xenobiotic compounds as well as for the tolerance of heavy metal ions. The isolate AK6 can be utilized for large-scale treatment of dye-containing effluents after the optimization study of

Table 3 Azoreductase and laccase genes identified in *P. stutzeri* genomes available in IMG/M

IMG/M Gene ID	Locus tag	Product name	Scaffold ID	Genome
Azoreductase gene (pfam02525 and COG1182)				
651019675	PSTAB_1543	NAD(P)H dehydrogenase (quinone)	NC_015740	*Pseudomonas stutzeri* CGMCC 1.1803
651175530	PSTAA_1661	NAD(P)H dehydrogenase (quinone)	CP002622	*Pseudomonas stutzeri* CMT.A.9, DSM 4166
2507212972	Psest_2740	FMN-dependent NADH-azoreductase	Psest_Contig47.1	*Pseudomonas stutzeri* RCH2
2516819675	A598_03134	FMN-dependent NADH-azoreductase	A598_gi396581749.114	*Pseudomonas stutzeri* XLDN-R
2516822380	PSTU_01305	FMN-dependent NADH-azoreductase	PSTU_gi357435889.54	*Pseudomonas stutzeri* SDM-LAC
2516826263	B319_01134	FMN-dependent NADH-azoreductase	B319_gi398363375.9	*Pseudomonas stutzeri* T13
2518857883	A458_08765	FMN-dependent NADH-azoreductase	CP003677	*Pseudomonas stutzeri* AN10, CCUG 29243
2520960728	PSJM300_07590	FMN-dependent NADH-azoreductase	CP003725	*Pseudomonas stutzeri* JM3000, DSM 10701
2520961932	PSJM300_13555	FMN-dependent NADH-azoreductase	CP003725	*Pseudomonas stutzeri* JM3000, DSM 10701
2525609456	PseudoMF28_02241	FMN-dependent NADH-azoreductase	PseudoMF28_gnl_FAMU_contig.17	*Pseudomonas stutzeri* MF28
2525609941	PseudoMF28_02726	FMN-dependent NADH-azoreductase	PseudoMF28_gnl_FAMU_contig.24	*Pseudomonas stutzeri* MF28
2531536751	PstZobell_05238	FMN-dependent NADH-azoreductase	AGSL01000045	*Pseudomonas stutzeri* ZoBell 632, ATCC 14405
2539728488	B381_05821	FMN-dependent NADH-azoreductase	AOBS01000034	*Pseudomonas stutzeri* NF13
2547111219	Ask1DRAFT_02785	FMN-dependent NADH-azoreductase	Ask1DRAFT_NODE_39_len_44029_cov_75_141838.36	*Pseudomonas stutzeri* ASK-1
2566244827	CH92_10210	FMN-dependent NADH-azoreductase	CP007441	*Pseudomonas stutzeri* 28a24
2566244953	CH92_10860	FMN-dependent NADH-azoreductase	CP007441	*Pseudomonas stutzeri* 28a24
2566245142	CH92_11825	FMN-dependent NADH-azoreductase	CP007441	*Pseudomonas stutzeri* 28a24
2566245695	CH92_14660	FMN-dependent NADH-azoreductase	CP007441	*Pseudomonas stutzeri* 28a24
2574575366	UIB01_13835	FMN-dependent NADH-azoreductase	CP007509	*Pseudomonas stutzeri* 19SMN4
2632719495	Ga0080851_1022	FMN-dependent NADH-azoreductase	Ga0080851_102	*Pseudomonas stutzeri* YC-YH1
2646853269	Ga0100546_102379	FMN-dependent NADH-azoreductase	Ga0100546_102	*Pseudomonas stutzeri* KF716
2649422080	Ga0100681_10747	FMN-dependent NADH-azoreductase	Ga0100681_1074	*Pseudomonas stutzeri* ST-9
2649632999	Ga0098632_115216	FMN-dependent NADH-azoreductase	Ga0098632_115	*Pseudomonas stutzeri* NT0128
2649633094	Ga0098632_1169	FMN-dependent NADH-azoreductase	Ga0098632_116	*Pseudomonas stutzeri* NT0128
2649633130	Ga0098632_11645	FMN-dependent NADH-azoreductase	Ga0098632_116	*Pseudomonas stutzeri* NT0128
2649634042	Ga0098632_12929	FMN-dependent NADH-azoreductase	Ga0098632_129	*Pseudomonas stutzeri* NT0128
2653331223	Ga0111029_124584	FMN-dependent NADH-azoreductase	Ga0111029_124	*Pseudomonas stutzeri* NP_8Ht
2653333624	Ga0111030_10997	FMN-dependent NADH-azoreductase	Ga0111030_109	*Pseudomonas stutzeri* NP_8HO
2655598144	Ga0100686_101110	FMN-dependent NADH-azoreductase	Ga0100686_101	*Pseudomonas stutzeri* NT0124
2674186373	Ga0112298_103823	FMN-dependent NADH-azoreductase	Ga0112298_1038	*Pseudomonas stutzeri* C2
2686649775	Ga0133288_113276	FMN-dependent NADH-azoreductase	Ga0133288_11	*Pseudomonas stutzeri* 273
2715898513	Ga0125715_109822	FMN-dependent NADH-azoreductase	Ga0125715_1098	*Pseudomonas stutzeri* BAL361
2730878807	Ga0127368_16782	FMN-dependent NADH-azoreductase	Ga0127368_167	*Pseudomonas stutzeri* ODKF13
2742120588	Ga0131013_1586130	FMN-dependent NADH-azoreductase	Ga0131013_1586	*Pseudomonas stutzeri* HI00D01

Table 3 (continued)

IMG/M Gene ID	Locus tag	Product name	Scaffold ID	Genome
2808545502	AK6_19660	FMN-dependent NADH-azoreductase	Contig_29_len_248786	*Pseudomonas stutzeri* AK6
Laccase-Multicopper oxidase-4 domain containing gene (pfam02578)				
640489583	PST_3641	Hypothetical protein	NC_009434	*Pseudomonas stutzeri* A1501
651021789	PSTAB_3607	Hypothetical protein	NC_015740	*Pseudomonas stutzeri* CGMCC 1.1803
651177607	PSTAA_3735	Conserved hypothetical protein	CP002622	*Pseudomonas stutzeri* CMT.A.9, DSM 4166
2507210943	Psest_0710	Conserved hypothetical protein	Psest_Contig47.1	*Pseudomonas stutzeri* RCH2
2516817637	A598_01092	Conserved hypothetical protein	A598_gi396581784.79	*Pseudomonas stutzeri* XLDN-R
2516822286	PSTU_01211	Conserved hypothetical protein	PSTU_gi357435897.50	*Pseudomonas stutzeri* SDM-LAC
2516825321	B319_00190	Conserved hypothetical protein	B319_gi398363387.3	*Pseudomonas stutzeri* T13
2518856764	A458_03235	Conserved hypothetical protein	CP003677	*Pseudomonas stutzeri* AN10, CCUG 29243
2520296473	B597_15923	Conserved hypothetical protein	AMCZ01000049	*Pseudomonas stutzeri* KOS6
2520959783	PSJM300_02985	Conserved hypothetical protein	CP003725	*Pseudomonas stutzeri* JM3000, DSM 10701
2525609394	PseudoMF28_02179	Conserved hypothetical protein	PseudoMF28_gnl_FAMU_contig.16	*Pseudomonas stutzeri* MF28
2531537907	PstZobell_11044	Conserved hypothetical protein	AGSL01000074	*Pseudomonas stutzeri* ZoBell 632, ATCC 14405
2532514533	YO5_07347	Conserved hypothetical protein	AJXE01000006	*Pseudomonas stutzeri* TS44
2539728050	B381_03657	Conserved hypothetical protein	AOBS01000021	*Pseudomonas stutzeri* NF13
2543259602	B382_02270	Conserved hypothetical protein	AMVM01000001	*Pseudomonas stutzeri* B1SMN1
2547110208	Ask1DRAFT_01773	Conserved hypothetical protein	Ask1DRAFT_NODE_24_len_294899_cov_99_147697.24	*Pseudomonas stutzeri* ASK-1
2566246314	CH92_17865	Conserved hypothetical protein	CP007441	*Pseudomonas stutzeri* 28a24
2574573254	UIB01_03020	Conserved hypothetical protein	CP007509	*Pseudomonas stutzeri* 19SMN4
2632721578	Ga0080851_106151	Conserved hypothetical protein	Ga0080851_106	*Pseudomonas stutzeri* YC-YH1
2646855471	Ga0100546_108127	Conserved hypothetical protein	Ga0100546_108	*Pseudomonas stutzeri* KF716
2649419804	Ga0100681_101591	Conserved hypothetical protein	Ga0100681_1015	*Pseudomonas stutzeri* ST-9
2649631852	Ga0098632_11154	Conserved hypothetical protein	Ga0098632_111	*Pseudomonas stutzeri* NT0128
2653329618	Ga0111029_123217	Hypothetical protein	Ga0111029_123	*Pseudomonas stutzeri* NP_8Ht
2653334952	Ga0111030_12189	Hypothetical protein	Ga0111030_121	*Pseudomonas stutzeri* NP_8HO
2655601942	Ga0100686_134165	Conserved hypothetical protein	Ga0100686_134	*Pseudomonas stutzeri* NT0124
2674186872	Ga0112298_10513	Conserved hypothetical protein	Ga0112298_1051	*Pseudomonas stutzeri* C2
2686650449	Ga0133288_113951	Conserved hypothetical protein	Ga0133288_11	*Pseudomonas stutzeri* 273
2715899640	Ga0125715_116522	Conserved hypothetical protein	Ga0125715_1165	*Pseudomonas stutzeri* BAL361
2730875280	Ga0127368_101513	Conserved hypothetical protein	Ga0127368_101	*Pseudomonas stutzeri* ODKF13
2742119162	Ga0131013_129630	Hypothetical protein	Ga0131013_1296	*Pseudomonas stutzeri* HI00D01
2808543012	AK6_07210	Hypothetical protein	Contig_11_len_262732	*Pseudomonas stutzeri* AK6
Laccase-multicopper oxidase with three cupredoxin domain gene (pfam07731 and pfam07732)				
640488950	PST_3006	Multicopper oxidase	NC_009434	*Pseudomonas stutzeri* A1501

Table 3 (continued)

IMG/M Gene ID	Locus tag	Product name	Scaffold ID	Genome
651021212	PSTAB_3044	Multicopper oxidase	NC_015740	*Pseudomonas stutzeri* CGMCC 1.1803
651177039	PSTAA_3168	Multicopper oxidase	CP002622	*Pseudomonas stutzeri* CMT.A.9, DSM 4166
2507211520	Psest_1288	Multicopper oxidase with three cupredoxin domains (includes cell division protein FtsP and spore coat protein CotA)	Psest_Contig47.1	*Pseudomonas stutzeri* RCH2
2516820816	A598_04275	Multicopper oxidase with three cupredoxin domains (includes cell division protein FtsP and spore coat protein CotA)	A598_gi396581703.160	*Pseudomonas stutzeri* XLDN-R
2516823230	PSTU_02156	Multicopper oxidase with three cupredoxin domains (includes cell division protein FtsP and spore coat protein CotA)	PSTU_gi357435791.103	*Pseudomonas stutzeri* SDM-LAC
2516828376	B319_03252	Multicopper oxidase with three cupredoxin domains (includes cell division protein FtsP and spore coat protein CotA)	B319_gi398363312.44	*Pseudomonas stutzeri* T13
2518857244	A458_05605	Multicopper oxidase with three cupredoxin domains (includes cell division protein FtsP and spore coat protein CotA)	CP003677	*Pseudomonas stutzeri* AN10, CCUG 29243
2520296830	B597_17840	Multicopper oxidase with three cupredoxin domains (includes cell division protein FtsP and spore coat protein CotA)	AMCZ01000052	*Pseudomonas stutzeri* KOS6
2520961833	PSJM300_13060	Multicopper oxidase with three cupredoxin domains (includes cell division protein FtsP and spore coat protein CotA)	CP003725	*Pseudomonas stutzeri* JM3000, DSM 10701
2525608220	PseudoMF28_01002	Multicopper oxidase with three cupredoxin domains (includes cell division protein FtsP and spore coat protein CotA)	PseudoMF28_gnl_FAMU_contig.6	*Pseudomonas stutzeri* MF28
2531537341	PstZobell_08240	Multicopper oxidase	AGSL01000063	*Pseudomonas stutzeri* ZoBell 632, ATCC 14405
2531538945	PstZobell_16341	Multicopper oxidase with three cupredoxin domains (includes cell division protein FtsP and spore coat protein CotA)	AGSL01000099	*Pseudomonas stutzeri* ZoBell 632, ATCC 14405
2532515357	YO5_08003	Multicopper oxidase with three cupredoxin domains (includes cell division protein FtsP and spore coat protein CotA)	AJXE01000013	*Pseudomonas stutzeri* TS44
2539728479	B381_05766	Multicopper oxidase with three cupredoxin domains (includes cell division protein FtsP and spore coat protein CotA)	AOBS01000033	*Pseudomonas stutzeri* NF13
2543261200	B382_10284	Multicopper oxidase with three cupredoxin domains (includes cell division protein FtsP and spore coat protein CotA)	AMVM01000005	*Pseudomonas stutzeri* B1SMN1

Table 3 (continued)

IMG/M Gene ID	Locus tag	Product name	Scaffold ID	Genome
2547111390	Ask1DRAFT_02956	Multicopper oxidase with three cupredoxin domains (includes cell division protein FtsP and spore coat protein CotA)	Ask1DRAFT_NODE_41_len_186451_cov_105_263107.38	*Pseudomonas stutzeri* ASK-1
2566245813	CH92_15285	Multicopper oxidase with three cupredoxin domains (includes cell division protein FtsP and spore coat protein CotA)	CP007441	*Pseudomonas stutzeri* 28a24
2574573844	UIB01_06010	Multicopper oxidase with three cupredoxin domains (includes cell division protein FtsP and spore coat protein CotA)	CP007509	*Pseudomonas stutzeri* 19SMN4
2632720687	Ga0080851_104305	Multicopper oxidase with three cupredoxin domains (includes cell division protein FtsP and spore coat protein CotA)	Ga0080851_104	*Pseudomonas stutzeri* YC-YH1
2632721182	Ga0080851_105331	Multicopper oxidase with three cupredoxin domains (includes cell division protein FtsP and spore coat protein CotA)	Ga0080851_105	*Pseudomonas stutzeri* YC-YH1
2646853372	Ga0100546_102482	Multicopper oxidase with three cupredoxin domains (includes cell division protein FtsP and spore coat protein CotA)	Ga0100546_102	*Pseudomonas stutzeri* KF716
2649420720	Ga0100681_102552	Multicopper oxidase with three cupredoxin domains (includes cell division protein FtsP and spore coat protein CotA)	Ga0100681_1025	*Pseudomonas stutzeri* ST-9
2649634165	Ga0098632_129152	Multicopper oxidase with three cupredoxin domains (includes cell division protein FtsP and spore coat protein CotA)	Ga0098632_129	*Pseudomonas stutzeri* NT0128
2653327727	Ga0111029_1041	FtsP/CotA-like multicopper oxidase with cupredoxin domain	Ga0111029_104	*Pseudomonas stutzeri* NP_8Ht
2653331318	Ga0111029_124679	FtsP/CotA-like multicopper oxidase with cupredoxin domain	Ga0111029_124	*Pseudomonas stutzeri* NP_8Ht
2655600378	Ga0100686_123159	Multicopper oxidase with three cupredoxin domains (includes cell division protein FtsP and spore coat protein CotA)	Ga0100686_123	*Pseudomonas stutzeri* NT0124
2674186120	Ga0112298_10336	Multicopper oxidase with three cupredoxin domains (includes cell division protein FtsP and spore coat protein CotA)	Ga0112298_1033	*Pseudomonas stutzeri* C2
2686649886	Ga0133288_113387	Multicopper oxidase with three cupredoxin domains (includes cell division protein FtsP and spore coat protein CotA)	Ga0133288_11	*Pseudomonas stutzeri* 273
2715900185	Ga0125715_123120	Multicopper oxidase with three cupredoxin domains (includes cell division protein FtsP and spore coat protein CotA)	Ga0125715_1231	*Pseudomonas stutzeri* BAL361

Table 3 (continued)

IMG/M Gene ID	Locus tag	Product name	Scaffold ID	Genome
2730878362	Ga0127368_156160	Multicopper oxidase with three cupredoxin domains (includes cell division protein FtsP and spore coat protein CotA)	Ga0127368_156	*Pseudomonas stutzeri* ODKF13
2742119587	Ga0131013_138085	FtsP/CotA-like multicopper oxidase with cupredoxin domain	Ga0131013_1380	*Pseudomonas stutzeri* HI00D01
2808544758	AK6_15940	FtsP/CotA-like multicopper oxidase with cupredoxin domain	Contig_24_len_349075	*Pseudomonas stutzeri* AK6
Laccase-copper-resistance protein family CopA gene (pfam00394, pfam07731 and pfam07732)				
640488659	PST_2715	Copper-resistance protein A precursor	NC_009434	*Pseudomonas stutzeri* A1501
640489325	PST_3383	Copper-resistance protein A	NC_009434	*Pseudomonas stutzeri* A1501
651020659	PSTAB_2502	Copper-resistance protein A	NC_015740	*Pseudomonas stutzeri* CGMCC 1.1803
651020858	PSTAB_2699	Copper-resistance protein A	NC_015740	*Pseudomonas stutzeri* CGMCC 1.1803
651176708	PSTAA_2837	Copper-resistance protein A precursor	CP002622	*Pseudomonas stutzeri* CMT.A.9, DSM 4166
651176825	PSTAA_2954	CopA family copper-resistance protein	CP002622	*Pseudomonas stutzeri* CMT.A.9, DSM 4166
651177396	PSTAA_3524	Copper-resistance protein A	CP002622	*Pseudomonas stutzeri* CMT.A.9, DSM 4166
2507210816	Psest_0583	Copper-resistance protein, CopA family	Psest_Contig47.1	*Pseudomonas stutzeri* RCH2
2507211822	Psest_1590	Copper resistance protein, CopA family	Psest_Contig47.1	*Pseudomonas stutzeri* RCH2
2516819317	A598_02776	Copper-resistance protein, CopA family	A598_gi396581758.105	*Pseudomonas stutzeri* XLDN-R
2516819776	A598_03235	Copper-resistance protein, CopA family	A598_gi396581748.115	*Pseudomonas stutzeri* XLDN-R
2516820619	A598_04078	Copper-resistance protein, CopA family	A598_gi396581716.147	*Pseudomonas stutzeri* XLDN-R
2516822488	PSTU_01413	Copper-resistance protein, CopA family	PSTU_gi357435877.60	*Pseudomonas stutzeri* SDM-LAC
2516828361	B319_03237	Copper-resistance protein, CopA family	B319_gi398363314.43	*Pseudomonas stutzeri* T13
2516828912	B319_03788	Copper-resistance protein, CopA family	B319_gi398363284.58	*Pseudomonas stutzeri* T13
2518858991	A458_14255	Copper-resistance protein, CopA family	CP003677	*Pseudomonas stutzeri* AN10, CCUG 29243
2518860435	A458_21445	Copper-resistance protein, CopA family	CP003677	*Pseudomonas stutzeri* AN10, CCUG 29243
2520293957	B597_02262	Copper-resistance protein, CopA family	AMCZ01000007	*Pseudomonas stutzeri* KOS6
2520294377	B597_04479	Copper-resistance protein, CopA family	AMCZ01000010	*Pseudomonas stutzeri* KOS6
2520294967	B597_07662	Copper-resistance protein, CopA family	AMCZ01000025	*Pseudomonas stutzeri* KOS6
2520295448	B597_10359	Copper-resistance protein, CopA family	AMCZ01000033	*Pseudomonas stutzeri* KOS6
2520961352	PSJM300_10695	Copper-resistance protein, CopA family	CP003725	*Pseudomonas stutzeri* JM3000, DSM 10701
2525608469	PseudoMF28_01251	Copper-resistance protein, CopA family	PseudoMF28_gnl_FAMU_contig.9	*Pseudomonas stutzeri* MF28
2525609978	PseudoMF28_02763	Copper-resistance protein, CopA family	PseudoMF28_gnl_FAMU_contig.24	*Pseudomonas stutzeri* MF28
2531536188	PstZobell_02396	Copper-resistance protein, CopA family	AGSL01000026	*Pseudomonas stutzeri* ZoBell 632, ATCC 14405
2531538378	PstZobell_13431	Copper-resistance protein, CopA family	AGSL01000080	*Pseudomonas stutzeri* ZoBell 632, ATCC 14405
2532514221	YO5_12927	Copper-resistance protein, CopA family	AJXE01000004	*Pseudomonas stutzeri* TS44
2532515308	YO5_07748	Copper-resistance protein, CopA family	AJXE01000013	*Pseudomonas stutzeri* TS44
2539727976	B381_03287	Copper-resistance protein, CopA family	AOBS01000021	*Pseudomonas stutzeri* NF13

Table 3 (continued)

IMG/M Gene ID	Locus tag	Product name	Scaffold ID	Genome
2539728185	B381_04327	Copper-resistance protein, CopA family	AOBS01000023	*Pseudomonas stutzeri* NF13
2539728845	B381_07606	Copper-resistance protein, CopA family	AOBS01000036	*Pseudomonas stutzeri* NF13
2543261381	B382_11186	Copper-resistance protein, CopA family	AMVM01000006	*Pseudomonas stutzeri* B1SMN1
2543262239	B382_15473	Copper-resistance protein, CopA family	AMVM01000010	*Pseudomonas stutzeri* B1SMN1
2547110314	Ask1DRAFT_01879	Copper-resistance protein, CopA family	Ask1DRAFT_NODE_24_len_294899_cov_99_147697.24	*Pseudomonas stutzeri* ASK-1
2547110951	Ask1DRAFT_02517	Copper-resistance protein, CopA family	Ask1DRAFT_NODE_34_len_347218_cov_99_159698.32	*Pseudomonas stutzeri* ASK-1
2547110952	Ask1DRAFT_02518	Copper-resistance protein, CopA family	Ask1DRAFT_NODE_34_len_347218_cov_99_159698.32	*Pseudomonas stutzeri* ASK-1
2566245655	CH92_14450	Copper-resistance protein, CopA family	CP007441	*Pseudomonas stutzeri* 28a24
2574574123	UIB01_07455	Copper-resistance protein, CopA family	CP007509	*Pseudomonas stutzeri* 19SMN4
2632721140	Ga0080851_105289	Copper-resistance protein, CopA family	Ga0080851_105	*Pseudomonas stutzeri* YC-YH1
2632722835	Ga0080851_11125	Copper-resistance protein, CopA family	Ga0080851_111	*Pseudomonas stutzeri* YC-YH1
2646853323	Ga0100546_102433	Copper-resistance protein, CopA family	Ga0100546_102	*Pseudomonas stutzeri* KF716
2646855588	Ga0100546_108244	Copper-resistance protein, CopA family	Ga0100546_108	*Pseudomonas stutzeri* KF716
2649419349	Ga0100681_10127	Copper-resistance protein, CopA family	Ga0100681_1012	*Pseudomonas stutzeri* ST-9
2649421878	Ga0100681_10587	Copper-resistance protein, CopA family	Ga0100681_1058	*Pseudomonas stutzeri* ST-9
2649422023	Ga0100681_10692	Copper-resistance protein, CopA family	Ga0100681_1069	*Pseudomonas stutzeri* ST-9
2649633805	Ga0098632_12488	Copper-resistance protein, CopA family	Ga0098632_124	*Pseudomonas stutzeri* NT0128
2653328349	Ga0111029_121296	CopA family copper-resistance protein	Ga0111029_121	*Pseudomonas stutzeri* NP_8Ht
2653331182	Ga0111029_124543	CopA family copper-resistance protein	Ga0111029_124	*Pseudomonas stutzeri* NP_8Ht
2655600128	Ga0100686_120368	Copper-resistance protein, CopA family	Ga0100686_120	*Pseudomonas stutzeri* NT0124
2674187020	Ga0112298_105616	Copper-resistance protein, CopA family	Ga0112298_1056	*Pseudomonas stutzeri* C2
2686649730	Ga0133288_113231	Copper-resistance protein, CopA family	Ga0133288_11	*Pseudomonas stutzeri* 273
2686649919	Ga0133288_113420	Copper-resistance protein, CopA family	Ga0133288_11	*Pseudomonas stutzeri* 273
2686651166	Ga0133288_114672	Copper-resistance protein, CopA family	Ga0133288_11	*Pseudomonas stutzeri* 273
2715896359	Ga0125715_100910	Copper-resistance protein, CopA family	Ga0125715_1009	*Pseudomonas stutzeri* BAL361
2715898224	Ga0125715_108611	Copper-resistance protein, CopA family	Ga0125715_1086	*Pseudomonas stutzeri* BAL361
2730878674	Ga0127368_156472	Copper-resistance protein, CopA family	Ga0127368_156	*Pseudomonas stutzeri* ODKF13
2742116958	Ga0131013_1010221	CopA family copper-resistance protein	Ga0131013_1010	*Pseudomonas stutzeri* HI00D01
2742118164	Ga0131013_10888	CopA family copper-resistance protein	Ga0131013_1088	*Pseudomonas stutzeri* HI00D01
2742119849	Ga0131013_147439	CopA family copper-resistance protein	Ga0131013_1474	*Pseudomonas stutzeri* HI00D01
2808545653	AK6_20415	CopA family copper-resistance protein	Contig_29_len_248786	*Pseudomonas stutzeri* AK6

environmental and nutritional parameters to achieve maximum decolorization with minimum requirements.

Acknowledgements We would like to thank DST (Department of Science and Technology) for the award of INSPIRE Fellowship (IF150437) to Anjali U. Joshi.

Author contributions Conceptualization: AJ, AH, data curation: AJ, formal analysis: AJ, investigation: AJ, methodology: AJ, RK, KA, software: AH, supervision: RK, validation: AJ, AH, writing—original draft: AJ, AH, writing—review and editing: AJ, JR, RK.

Compliance with ethical standards

Conflict of interest The authors declare no conflict of interest.

References

Ajaz M, Elahi A, Rehman A (2018) Degradation of azo dye by bacterium, Alishewanella sp. CBL-2 isolated from industrial effluent and its potential use in decontamination of wastewater. J Water Reuse Desal 8(4):507–515

Ajaz M, Rehman A, Khan Z, Nisar MA, Hussain S (2019) Degradation of azo dyes by Alcaligenes aquatilis 3c and its potential use in the wastewater treatment. AMB Express 9(1):64

Alalewi A, Jiang C (2012) Bacterial influence on textile wastewater decolorization. J Environ Prot 3(08):889

Aquino JM, Rocha-Filho RC, Ruotolo LA, Bocchi N, Biaggio SR (2014) Electrochemical degradation of a real textile wastewater using β-PbO2 and DSA® anodes. Chem Eng J 251:138–145

Bafana A, Devi SS, Krishnamurthi K, Chakrabarti T (2007) Kinetics of decolourisation and biotransformation of direct black 38 by *C. hominis* and *P. stutzeri*. Appl Microbiol Biotechnol 74(5):1145–1152

Banat IM, Nigam P, Singh D, Marchant R (1997) Microbial decolorization of textile-dye-containing effluents: a review (vol 58, pg 217, 1996). Bioresour Technol 61(1):103–103

Bankevich A, Nurk S, Antipov D, Gurevich AA, Dvorkin M, Kulikov AS, Lesin VM, Nikolenko SI, Pham S, Prjibelski AD (2012) SPAdes: a new genome assembly algorithm and its applications to single-cell sequencing. J Comput Biol 19(5):455–477

Bhavsar S, Dudhagara P, Tank S (2018) R software package based statistical optimization of process components to simultaneously enhance the bacterial growth, laccase production and textile dye decolorization with cytotoxicity study. PLoS ONE 13(5):e0195795

Brunet-Galmés I, Busquets A, Peña A, Gomila M, Nogales B, García-Valdés E, Lalucat J, Bennasar A, Bosch R (2012) Complete genome sequence of the naphthalene-degrading bacterium Pseudomonas stutzeri AN10 (CCUG 29243). J Bacteriol 194(23):6642–6643

Bushnell L, Haas H (1941) The utilization of certain hydrocarbons by microorganisms. J Bacteriol 41(5):653

Busquets A, Peña A, Gomila M, Mayol J, Bosch R, Nogales B, García-Valdés E, Bennasar A, Lalucat J (2013) Draft genome sequence of Pseudomonas stutzeri strain B1SMN1, a nitrogen-fixing and naphthalene-degrading strain isolated from wastewater. Genome Announc 1(4):e00513–e00584

Chan GF, Rashid NA, Koay LL, Chang SY, Tan WL (2011) Identification and optimization of novel NAR-1 bacterial consortium for the biodegradation of Orange II. Insight Biotechnol 1(1):7–16

Chang J-S, Kuo T-S (2000) Kinetics of bacterial decolorization of azo dye with *Escherichia coli* NO3. Bioresour Technol 75(2):107–111

Chavan RB (2001) Indian textile industry-environmental issues. Indian J Fibre Text Res 26(1–2):11–21

Chen H, Hopper SL, Cerniglia CE (2005) Biochemical and molecular characterization of an azoreductase from Staphylococcus aureus, a tetrameric NADPH-dependent flavoprotein. Microbiology 151(5):1433–1441

Christie JM (2007) Phototropin blue-light receptors. Annu Rev Plant Biol 58:21–45

Copaciu F, Opriş O, Coman V, Ristoiu D, Niinemets Ü, Copolovici L (2013) Diffuse water pollution by anthraquinone and azo dyes in environment importantly alters foliage volatiles, carotenoids and physiology in wheat (*Triticum aestivum*). Water Air Soil Pollut 224(3):1478

Denisov G, Walenz B, Halpern AL, Miller J, Axelrod N, Levy S, Sutton G (2008) Consensus generation and variant detection by Celera Assembler. Bioinformatics 24(8):1035–1040

Dutta AK, Maji SK, Adhikary B (2014) γ-Fe2O3 nanoparticles: an easily recoverable effective photo-catalyst for the degradation of rose bengal and methylene blue dyes in the waste-water treatment plant. Mater Res Bull 49:28–34

Enayatzamir K, Tabandeh F, Yakhchali B, Alikhani HA, Couto SR (2009) Assessment of the joint effect of laccase and cellobiose dehydrogenase on the decolouration of different synthetic dyes. J Hazard Mater 169(1–3):176–181

Ghodake G, Jadhav U, Tamboli D, Kagalkar A, Govindwar S (2011) Decolorization of textile dyes and degradation of mono-azo dye amaranth by *Acinetobacter calcoaceticus* NCIM 2890. Indian J Microbiol 51(4):501–508

Gurevich A, Saveliev V, Vyahhi N, Tesler G (2013) QUAST: quality assessment tool for genome assemblies. Bioinformatics 29(8):1072–1075

Hirose J, Yamazoe A, Hosoyama A, Kimura N, Suenaga H, Watanabe T, Fujihara H, Futagami T, Goto M, Furukawa K (2015) Draft genome sequence of the polychlorinated biphenyl-degrading bacterium Pseudomonas stutzeri KF716 (NBRC 110668). Genome Announc 3(5):e01215–01215

Iyer R, Damania A (2016) Draft genome sequence of *Pseudomonas stutzeri* ODKF13, isolated from farmland soil in Alvin. Texas Genome Announc 4(2):e00216–e293

Jadhav J, Parshetti G, Kalme S, Govindwar S (2007) Decolourization of azo dye methyl red by *Saccharomyces cerevisiae* MTCC 463. Chemosphere 68(2):394–400

Jin R-f, Zhou J-t, Zhang A-l, Wang J (2008) Bioaugmentation of the decolorization rate of acid red GR by genetically engineered microorganism *Escherichia coli* JM109 (pGEX-AZR). World J Microb Biot 24(1):23–29

Kadam AA, Telke AA, Jagtap SS, Govindwar SP (2011) Decolorization of adsorbed textile dyes by developed consortium of Pseudomonas sp. SUK1 and *Aspergillus ochraceus* NCIM-1146 under solid state fermentation. J Hazard Mater 189(1–2):486–494

Kalme S, Jadhav S, Jadhav M, Govindwar S (2009) Textile dye degrading laccase from Pseudomonas desmolyticum NCIM 2112. Enzyme Microb Technol 44(2):65–71

Khalid A, Arshad M, Crowley DE (2008) Accelerated decolorization of structurally different azo dyes by newly isolated bacterial strains. Appl Microbiol Biotechnol 78(2):361–369

Khalid A, Arshad M, Crowley DE (2009) Biodegradation potential of pure and mixed bacterial cultures for removal of 4-nitroaniline from textile dye wastewater. Water Res 43(4):1110–1116

Khan S, Malik A (2018) Toxicity evaluation of textile effluents and role of native soil bacterium in biodegradation of a textile dye. Environ Sci Pollut Res 25(5):4446–4458

Khatri J, Nidheesh P, Singh TA, Kumar MS (2018) Advanced oxidation processes based on zero-valent aluminium for treating textile wastewater. Chem Eng J 348:67–73

Kieser T, Bibb M, Buttner M, Chater K, Hopwood D (2000) Practical streptomyces genetics. The John Innes Foundation, Norwich

Kuppusamy S, Sethurajan M, Kadarkarai M, Aruliah R (2017) Biodecolourization of textile dyes by novel, indigenous *Pseudomonas stutzeri* MN1 and *Acinetobacter baumannii* MN3. J Environ Chem Eng 5(1):716–724

Lalucat J, Bennasar A, Bosch R, García-Valdés E, Palleroni NJ (2006) Biology of *Pseudomonas stutzeri*. Microbiol Mol Biol Rev 70(2):510–547

Liao Y-C, Lin H-H, Sabharwal A, Haase EM, Scannapieco FA (2015) MyPro: a seamless pipeline for automated prokaryotic genome assembly and annotation. J Microbiol Methods 113:72–74

Lin J, Zhang X, Li Z, Lei L (2010) Biodegradation of Reactive blue 13 in a two-stage anaerobic/aerobic fluidized beds system with a Pseudomonas sp. isolate. Bioresour Technol 101(1):34–40

Lin S-H, Liao Y-C (2013) CISA: contig integrator for sequence assembly of bacterial genomes. PLoS ONE 8(3):e60843

Liu X, Gai Z, Tao F, Yu H, Tang H, Xu P (2012) Genome sequences of *Pseudomonas luteola* XLDN4-9 and *Pseudomonas stutzeri* XLDN-R, two efficient carbazole-degrading strains. J Bacteriol 194(20):5701–5702

Majcherczyk A, Johannes C, Hüttermann A (1998) Oxidation of polycyclic aromatic hydrocarbons (PAH) by laccase of *Trametes versicolor*. Enzyme Microb Technol 22(5):335–341

Mehta P, Mehta R, Surana M, Kabra B (2011) Influence of operational parameters on degradation of commercial textile azo dye acid blue 113 (cyanine 5r) by advanced oxidation technology. J Curr Chem Pharm Sci 1(1):28–36

Nachiyar CV, Rajakumar GS (2005) Purification and characterization of an oxygen insensitive azoreductase from *Pseudomonas aeruginosa*. Enzyme Microb Technol 36(4):503–509

O'Neill C, Hawkes FR, Hawkes DL, Lourenço ND, Pinheiro HM, Delée W (1999) Colour in textile effluents–sources, measurement, discharge consents and simulation: a review. J Chem Technol Biotechnol Int Res Process Environ Clean Technol 74(11):1009–1018

Pandey A, Singh P, Iyengar L (2007) Bacterial decolorization and degradation of azo dyes. Int Biodeterior Biodegrad 59(2):73–84

Park E-H, Jang M-S, Cha I-H, Choi Y-L, Cho Y-S, Kim C-H, Lee Y-C (2005) Decolorization of a sulfonated azo dye, Congo Red, by Staphylococcus sp. EY-3. J Microbiol Biotechn 15(1):221–225

Parks DH, Imelfort M, Skennerton CT, Hugenholtz P, Tyson GW (2015) CheckM: assessing the quality of microbial genomes recovered from isolates, single cells, and metagenomes. Genome Res:gr 186072:186114

Parshetti G, Kalme S, Saratale G, Govindwar S (2006) Biodegradation of Malachite Green by Kocuria rosea MTCC 1532. Acta Chimica Slovenica 53(4):492–498

Pillai HJS (2017) Optimization of process conditions for effective degradation of azo Blue Dye by streptomyces DJP15. J Pure Appl Microbiol 11(4):9

Predescu A, Nicolae A (2012) Adsorption of Zn, Cu and Cd from waste waters by means of maghemite nanoparticles. UPB Buletin Stiintific, Ser B Chem Mater Sci 74(1):255–264

Qi J, Wang B, Hao B-I (2004) Whole proteome prokaryote phylogeny without sequence alignment: a K-string composition approach. J Mol Evol 58(1):1–11

Robinson T, McMullan G, Marchant R, Nigam P (2001) Remediation of dyes in textile effluent: a critical review on current treatment technologies with a proposed alternative. Bioresour Technol 77(3):247–255

Roy DC, Biswas SK, Saha AK, Sikdar B, Rahman M, Roy AK, Prodhan ZH, Tang S-S (2018) Biodegradation of Crystal Violet dye by bacteria isolated from textile industry effluents. PeerJ 6:e5015

Sarayu K, Sandhya S (2010) Aerobic biodegradation pathway for Remazol Orange by *Pseudomonas aeruginosa*. Appl Biochem Biotechnol 160(4):1241–1253

Shi Y-h, Ren L, Jia Y, Yan Y-c (2015) Genome sequence of organophosphorus pesticide-degrading bacterium *Pseudomonas stutzeri* strain YC-YH1. Genome Announc 3(2):e00115–e00192

Soft C (2001) ChemDraw Ultra. Cambridge Soft Corporation, Cambridge

Solís M, Solís A, Pérez HI, Manjarrez N, Flores M (2012) Microbial decolouration of azo dyes: a review. Process Biochem 47(12):1723–1748

Tatusova T, DiCuccio M, Badretdin A, Chetvernin V, Nawrocki EP, Zaslavsky L, Lomsadze A, Pruitt KD, Borodovsky M, Ostell J (2016) NCBI prokaryotic genome annotation pipeline. Nucleic Acids Res 44(14):6614–6624

Ulson SMdAG, Bonilla KAS, de Souza AAU (2010) Removal of COD and color from hydrolyzed textile azo dye by combined ozonation and biological treatment. J Hazard Mater 179(1–3):35–42

Vankar PS (2016) Handbook on natural dyes for industrial applications (extraction of dyestuff from flowers, leaves, vegetables): How to start a natural dyes Sector?, How to start a successful natural dyes business, How to start natural dyes production Industry in India, Information on Natural Dyes, Make Natural Dyes for Dyeing, Making Natural Dyes from Plants, Most Profitable natural dyes Business Ideas. NIIR PROJECT CONSULTANCY SERVICES

Zerbino D, Birney E (2008) Velvet: algorithms for de novo short read assembly using de Bruijn graphs. Genome Res:gr 074492:074107

Zuo G, Hao B (2015) CVTree3 web server for whole-genome-based and alignment-free prokaryotic phylogeny and taxonomy. Genomics Proteomics Bioinf 13(5):321–331